

# Optimized PID Controller of DC-DC Buck Converter based on Archimedes Optimization Algorithm

Ling Kuok Fong <sup>a,1</sup>, Muhammad Shafiqul Islam <sup>b,2</sup>, Mohd Ashraf Ahmad <sup>c,3\*</sup>

<sup>a</sup> Faculty of Electrical and Electronics Engineering Technology, Universiti Malaysia Pahang Al-Sultan Abdullah, Pekan, 26600, Malaysia

<sup>b</sup> Faculty of Electrical and Electronics Engineering Technology, Universiti Malaysia Pahang Al-Sultan Abdullah, Pekan, 26600, Malaysia

<sup>c</sup> Centre for Advanced Industrial Technology, Universiti Malaysia Pahang Al-Sultan Abdullah, Pekan, 26600, Malaysia

<sup>1</sup> [lingkuokfong@gmail.com](mailto:lingkuokfong@gmail.com); <sup>2</sup> [msi.pust.bd@gmail.com](mailto:msi.pust.bd@gmail.com); <sup>3</sup> [mashraf@ump.edu.my](mailto:mashraf@ump.edu.my)

\* Corresponding Author

## ARTICLE INFO

## ABSTRACT

### Article history

Received August 09, 2023

Revised September 11, 2023

Accepted September 23, 2023

### Keywords

Buck Converter;

PID Controller;

Metaheuristic Algorithm;

Optimization

This research assesses the suitability of the Archimedes Optimization Algorithm (AOA) as a metaheuristic technique to fine-tune a PID controller in a closed-loop DC-DC buck converter. The converter's core function is to regulate output voltage, ensuring stability despite load fluctuations and input voltage changes. The operational effectiveness of the converter hinges significantly on the gain settings of the PID controller and determining the optimal gain setting for the PID controller is a non-trivial task. For robust performance, the PID controller necessitates optimal gain settings, attainable through metaheuristic optimization. The algorithm aids in identifying ideal proportional, integral, and derivative gains based on varying load conditions. Leveraging the metaheuristic algorithm, the PID controller is optimized to minimize voltage errors, reduce overshoot, and enhance response time. The proposed PID controller, optimized using AOA, is contrasted with PID controllers tuned via alternative algorithms including the hybrid Nelder-Mead method (AEONM), artificial ecosystem-based optimization (AEO), differential evolution (DE), and particle swarm optimizer (PSO). Performance evaluation involves injecting a voltage disturbance into the buck converter with load changes of up to 20%. Results demonstrate the superiority of the AOA-optimized PID controller in voltage recovery. It demonstrates a faster response time and outstanding voltage regulation performance, while also exhibiting minimal performance degradation during load changes. This study concludes that the AOA optimization algorithm surpasses other methods in tuning the PID controller for closed-loop DC-DC buck converters.

This is an open-access article under the [CC-BY-SA](https://creativecommons.org/licenses/by-sa/4.0/) license.



## 1. Introduction

The DC-DC buck converter stands as a fundamental component in diverse electronic systems, offering voltage stabilization for equipment [1]. Its applications span across consumer electronics, telecommunications, electric vehicles, renewable energy systems, and more, where it serves as a power supply, battery charge controller, and voltage level converter [2]–[6]. This versatile role highlights its significance in powering electronics across industries.

In the realm of control strategies for buck converters, several approaches have been explored. However, due to its simplicity, adaptability, and effectiveness in handling nonlinearities, the Proportional-Integral-Derivative (PID) controller has emerged as a preferred choice [7]. While existing studies have focused on various control methodologies [8]–[18], we find that the PID controller's straightforward structure offers a compelling solution for managing the buck converter's dynamic behavior.

The previous study about the disturbance analysis on the buck converter focused on input voltage variability and the injection of disturbance voltages [1], [11], [19]–[21]. In the presence of voltage fluctuations or disturbances, the primary objective of a buck converter is to sustain a stable output voltage without being affected by the disturbance. However, in practical scenarios, buck converters are susceptible to disturbances, resulting in a temporary deviation of the output voltage from its desired level. This behavior arises due to the inherent characteristics of the feedback loop, where the voltage control is based on the output voltage error. Consequently, the disturbance-induced voltage error occurs initially, and then the controller takes corrective action to restore the output voltage to its intended level.

In order to address the effects of voltage fluctuations and disturbances on the load, it is essential to perform precise tuning of the closed-loop PID controller to achieve optimal performance. However, determining the optimal gain settings for the PID controller can be challenging due to the nonlinearity of the buck converter [22]. Various methods have been employed to identify the optimal PID gain settings, including the Ziegler-Nichols method [23]–[25], Cohen-Coon method [26]–[28], trial and error method [25], [29], and auto-tuning method [30]. While the Ziegler-Nichols and Cohen-Coon methods are more suitable for linear systems as they rely on mathematical formulas developed for such systems. The auto-tuning method offers a greater potential for achieving improved system performance in nonlinear systems. This method involves iterative testing of different PID gains until a satisfactory outcome is obtained, with the aid of an algorithm to determine the optimal PID gains.

Given the diverse range of loads that the buck converter is employed for an efficient algorithm is necessary to optimize the PID controller based on the specific load conditions. Consequently, the PID controller settings will vary depending on the load and buck converter. The PID controller consists of three gains: proportional gain, integral gain, and derivative gain, each of which can be assigned different values. Previous studies have utilized various algorithms, such as Genetic Algorithm [31], modified Lévy Flight Distribution Algorithm [32], Whale Optimization Algorithm [33], Firefly Algorithm [34], [35], Hybrid Firefly and Particle Swarm Optimization Algorithm [36], Chaotic flower pollination algorithm [37], Hybrid Whale Optimization Algorithm [38], Bat Algorithm [39], Sine Cosine Algorithm [40], Hybrid Nelder-Mead method [20], Antlion Optimization Algorithm [41], Cohort Intelligent Algorithm [42], Coevolving-AMOSA Algorithm [43] and improved Marine Predators Algorithm [44] to determine the optimal gain settings of PID controller.

Our study is motivated by the need for an effective and adaptable optimization technique for PID controllers in buck converters. AOA, known for its success in diverse optimization problems [45]–[49], holds promise in this context. By applying AOA, we seek to fine-tune the PID controller and compare its performance with existing algorithms like AEONM, AEO, PSO, and DE [20]. The benchmarks include comprehensive performance evaluations encompassing response analysis, statistical assessments, time response specifications, frequency response analysis, disturbance rejection, and parameter uncertainty analysis. The research contribution is:

- i. Evaluating the performance of a PID controller tuned by AOA in mitigating voltage disturbances in a buck converter, in comparison to other existing algorithms such as AEONM, AEO, PSO, and DE, as discussed in [20].
- ii. Examining the PID controller's robustness to a load change of 20%.
- iii. Frequency analysis on the PID controller

## 2. Method

### 2.1. PID Controller of DC-DC Buck Converter

The DC-DC buck converter is a power electronics device that converts a higher voltage input to a lower voltage output. The operation of the converter involves switching on and off a power semiconductor device, such as a MOSFET or an IGBT, at a high frequency to control the output voltage. The converter was constructed using various components such as switch ( $S$ ), diode ( $D$ ), inductor ( $L$ ), and capacitor ( $C$ ). This study considers the resistor ( $R$ ) as the load in the converter. The schematic diagram of the DC-DC buck converter utilized in the study can be seen in Fig. 1, where  $V_{in}$  is the input voltage and  $V_{out}$  is the load's voltage.

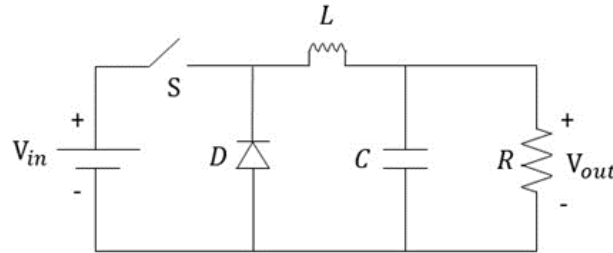


Fig. 1. DC-DC buck converter schematic diagram

In this study, each parameter employed in the converter is the same value in the paper [20]. Table 1 displays each parameter's value.

Table 1. DC-DC buck converter parameters value

Parameter	Value
$V_{in}$	36v
$V_{out}$	3v
$R$	6 $\Omega$
$L$	1mH
$C$	100 $\mu$ F

To design a closed-loop DC-DC buck converter, it is necessary to first derive the DC-DC buck converter's transfer function. Because the converter exhibits nonlinear behavior, obtaining its transfer function is a difficult task. Hence, this study adopted the formula to calculate the gain of the DC-DC buck converter ( $G_{bc}$ ) from paper [20], which is demonstrated in (1).

$$G_{bc} = V_{in} \times \frac{1/LC}{s^2 + s/RC + 1/RC} \quad (1)$$

By substituting the values from Table 1 into (1), the gain of the DC-DC converter can be determined and shown in (2).

$$G_{bc} = \frac{216000}{0.0006s^2 + s + 6000} \quad (2)$$

There are three control parameters in the gain equation of the PID controller, namely proportional gain ( $K_p$ ), integral gain ( $K_i$ ), and derivative gain ( $K_d$ ). The optimum value of those three parameters will be found using some different optimization algorithms to achieve the best possible response time with minimum voltage error and voltage overshoot. Equation (3) presents the transfer function of the PID controller and its corresponding  $K_p$ ,  $K_i$ , and  $K_d$  gains.

$$G_{controller} = K_p + \frac{K_i}{s} + K_d s \quad (3)$$

To analyze the transient response of the closed-loop PID-controlled DC-DC buck converter, it is necessary to obtain the closed-loop system transfer function. The closed-loop block diagram of the PID controller for the DC-DC buck converter, which was taken from [20] is shown in Fig. 2.

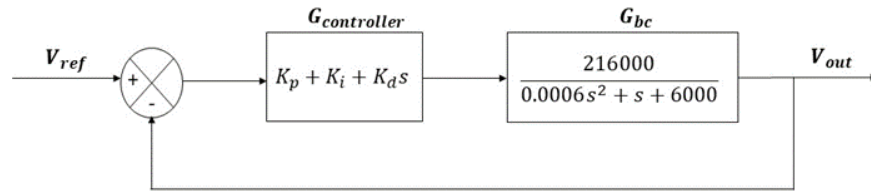


Fig. 2. Feedback loop of PID-controlled DC-DC buck converter

Since the model is in a feedback form, the closed-loop transfer function  $TF_{closed-loop}$  can easily solve by using (4).

$$TF_{closed-loop} = \frac{G_{bc} \times G_{controller}}{1 + G_{bc} \times G_{controller}} \quad (4)$$

After obtaining the closed-loop transfer function formula, different gain values of the PID controller can be applied to the formula for step response analysis. The important parameters in disturbance injection analysis such as rise period, settling period, voltage overshoot, and steady-state error can be found through the closed-loop transfer function. This analysis is useful for evaluating the performance of the closed-loop system under different PID controller parameter values.

## 2.2. Self-Tuning PID Controller of DC-DC Buck Converter

In this section, the process of applying the Archimedes Optimization Algorithm (AOA) to fine-tune the DC-DC buck converter's PID controller will be discussed. The mathematical structure and the step-by-step guide for the implementation will be presented. Hashim et al. proposed an alternative algorithm called the Archimedes optimization algorithm (AOA) for solving the Congress on Evolutionary Computation (CEC), engineering, and standard optimization problem [50]. The AOA is a metaheuristic method based on Archimedes' principle, which explains the relationship between a fluid-immersed object and the buoyant force applied to it. This algorithm has been shown to outperform other popular metaheuristic methods such as PSO, GA, SCA, and EO in multiple benchmark tests due to its simple structure and a smaller number of coefficients. The AOA follows a step-by-step procedure, which is outlined below:

Step 1-*Object initialization*: All objects' positions are initialized using (5).

$$x_i = lb_i + rand \times (ub_i - lb_i) \quad (5)$$

For  $i = 1, 2, \dots, n$ , where  $x_i$  is the  $i$ th object's position in a population with  $n$  number of objects. The upper and lower bounds of search space are represented by the symbols  $ub_i$  and  $lb_i$ , respectively. The  $i$ th objects' density ( $den$ ), volume ( $vol$ ), and acceleration ( $acc$ ) are initialized using (6).

$$den_i = rand,$$

$$vol_i = rand,$$

$$acc_i = lb_i + rand \times (ub_i - lb_i) \quad (6)$$

Where  $rand$  is a random vector of a number between  $[0, 1]$ .

Step 2-*Update object's volume and density*: The updated density and volume in next iteration are given by (7).

$$\begin{aligned} den_i^{k+1} &= den_i^k + rand \times (den_{best} - den_i^k) \\ vol_i^{k+1} &= vol_i^k + rand \times (vol_{best} - vol_i^k) \end{aligned} \quad (7)$$

Where  $k$  is the iteration number,  $den_{best}$  and  $vol_{best}$  are the best object's density, and volume found so far, and  $rand$  is another random vector of a number between  $[0, 1]$ .

Step 3-*Calculate transfer operator and density factor*: The objects attempt to attain an equilibrium condition after initially colliding with one another. Transfer operator  $TF$  shown in (8), which changes the search from exploration to exploitation, is used in AOA to execute this.

$$TF = \exp\left(\frac{k - k_{max}}{k_{max}}\right) \quad (8)$$

Where  $k_{max}$  is the maximum number of iterations.  $TF$  will gradually increased over iteration and until it reaches 1. Moreover, the density decreasing factor,  $d$ , helps AOA does for local to global search, which is expressed using (9).

$$d^{k+1} = \exp\left(\frac{k_{max} - k}{k_{max}}\right) - \left(\frac{k}{k_{max}}\right) \quad (9)$$

Where  $d^{k+1}$  decreases with iteration that enables convergence in a previously determined promising zone. It should be noted that effective management of  $TF$  and  $d$  will provide between AOA's exploration and exploitation.

Step 4.1- *Verity exploration phase*: If  $TF \leq 0.5$ , a collision between objects occurs. Then, a random material  $mr$  is selected, and the acceleration of object is updated for iteration  $k + 1$  using (10).

$$acc_i^{k+1} = \frac{den_{mr} + vol_{mr} \times acc_{mr}}{den_i^{k+1} \times vol_i^{k+1}} \quad (10)$$

Where  $den_{mr}$ ,  $vol_{mr}$ , and  $acc_{mr}$  are the density, volume, and acceleration of the  $i$ th object.

Step 4.2-*Verity exploitation phase*: On the other hand, if  $TF > 0.5$ , there is no collision between objects. Then, acceleration of object is updated for iteration  $k + 1$  using (11).

$$acc_i^{k+1} = \frac{den_{mr} + vol_{mr} \times acc_{best}}{den_i^{k+1} \times vol_i^{k+1}} \quad (11)$$

Where  $acc_{best}$  is the acceleration of the best object.

Step 4.3- *Calculate normalize acceleration*: The normalize acceleration is performed using (12) to calculate the percentage of change:

$$acc_{i-norm}^{k+1} = u \times \frac{acc_i^{k+1} - \min(acc)}{\max(acc) - \min(acc)} + l \quad (12)$$

Where  $u$  and  $l$  are the range of normalization, which is set to 0.9 and 0.1, respectively. The  $acc_{i-norm}^{k+1}$  determines the percentage change of each object's step. The acceleration value will be low if the object is near the global optimum, suggesting the object is in the exploitation phase. If not, it is still in the exploration stage. This shows how the search agent changes from exploration to exploitation phase.

Step5-*Update object's position*: If  $TF \leq 0.5$ , the  $i$ th object's position is updated using (13).

$$x_i^{k+1} = x_i^k + C_1 \times rand \times acc_{i-norm}^{k+1} \times (x_{rand} - x_i^k) \times d \quad (13)$$

Where  $C_1$  is a constant that equals to 2,  $x_{rand}$  is a random object's position, and  $rand$  is a random vector of a number between  $[0, 1]$ . If  $TF > 0.5$ , the object's position is instead updated using (14).

$$x_i^{k+1} = x_{best} \times F \times C_2 \times rand \times acc_{i-norm}^{k+1} \times (T \times x_{best} - x_i^k) \times d \quad (14)$$

Where  $x_{best}$  is the best object's position and  $C_2$  is a constant that equals 6. Here, the variable  $T$  is defined by  $T = C_3 \times T$ , where  $C_3$  is a constant that equals 2. Note that  $T$  increases with each iteration and has a range of  $[C_3 \times 0.3, 1]$ . In (13), the direction of the motion is handled by the flag  $F$  is using (15).

$$F = \begin{cases} +1 & \text{if } Pr \leq 0.5 \\ -1 & \text{if } Pr > 0.5 \end{cases} \quad (15)$$

For  $Pr = 2 \times rand - C_4$ , where  $C_4$  is a constant that equals 0.5 and  $rand$  is a random vector of a number between  $[0, 1]$ .

Step 6- *Object's position evaluation*: Finally, evaluate each object's position using objective function and saves the best solutions found so far that are corresponded to the best solution  $x_{best}$ ,  $den_{best}$ ,  $vol_{best}$ , and  $acc_{best}$ .

Fig. 3 displays the pseudocode of the AOA and Fig. 4 displays the flowchart of the AOA, which outlines the sequence of steps to be followed in a clear and concise manner.

### 2.3. The Application of AOA for PID Tuning of DC-DC Buck Converter

This section will explore the implementation of the Archimedes Optimization Algorithm (AOA) to tune the PID controller of a DC-DC buck converter using the MATLAB software. An objective function was used to evaluate the quality of a solution and guide the algorithm toward finding the best solution possible. The objective function is a key component in optimization algorithms and is typically defined by the problem being solved. The objective function of the DC-DC buck converter,  $J$  is based on the paper of [20] and is shown in (16).

$$J = (1 - e^{-\sigma}) \times (M_p + E_{ss}) + e^{-\sigma} \times (T_s - T_r) \quad (16)$$

Where  $M_p$  is percentage of voltage overshoot,  $E_{ss}$  is steady-state error,  $T_s$  is setting period and  $T_r$  is rising period. The  $\sigma$  is a constant, which is set as  $5 \times 10^{-5}$ . In this study, a lower value of the objective function indicates better performance of the DC-DC buck converter in step response analysis. The rising period, settling period, overshoot, and steady-state error are all proportional to the objective function in this study, and the converter is considered to have better performance when these parameters have lower values. Therefore, a lower value of the objective function is indicative of better system performance and MATLAB program will find the lowest values. The following is a step-by-step procedure for tuning the PID controller of the DC-DC buck converter using AOA.

Step 1: Identity the population size ( $n$ ) and maximum number of iterations ( $k_{max}$ ).

Step 2: Execute the AOA method in the pseudocode of Fig. 3 and use (16) to evaluate the objective function of each object's position. Here, the PID parameters are defined as the object's position.

Step 3: When  $k_{max}$  is reached, the best object's position is the result of PID controller tuning parameters.

To be fair compared with other algorithms in paper [20], the above step was run separately 25 times, and the results were saved after each run. The optimal tuning parameters for the PID controller, as tuned by the AOA, will be based on the best result obtained from these 25 independent runs.

**Algorithm 1** Pseudocode of AOA.

---

**Procedure** AOA (population size  $n$ , upper bound  $ub_i$ , lower bound  $lb_i$ , maximum iterations  $k_{max}$ ,  $C_1$ ,  $C_2$ ,  $C_3$ , and  $C_4$ )

Initialize objects population with random positions, densities and volumes using Eq. (4) and Eq. (5) respectively

Evaluate initial population and select the one with the best fitness value.

Set iteration counter  $k=1$

**while**  $k \leq k_{max}$  **do**

**for** each object  $i$  **do**

    Update density and volume of each object using Eq. (6)

    Update transfer and density decreasing factors  $TF$  and  $d$  using Eq. (7) and Eq. (8), respectively.

**if**  $TF \leq 0.5$  **then** →Exploration phase

      Update acceleration using Eq. (9) and normalize acceleration using Eq. (11)

      Update position using Eq. (12)

**else** →Exploitation phase

      Update acceleration using Eq. (10) and normalize acceleration using Eq. (11)

      Update direction flag  $F$  using Eq. (14)

      Update position using Eq. (13)

**end if**

**end for**

Evaluate each object and select the one with the best fitness value.

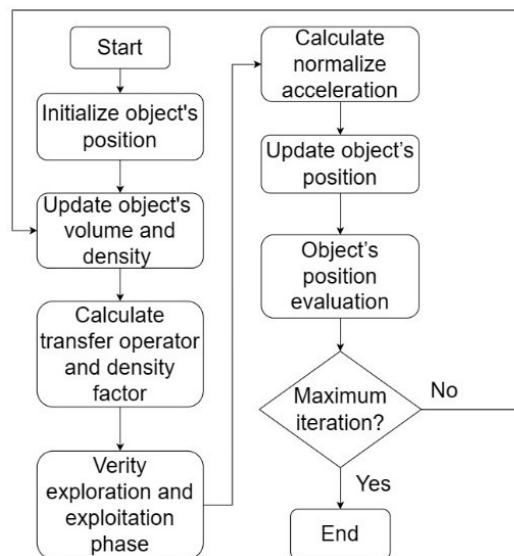
Set  $k = k + 1$

**end while**

**return** object with best fitness value

end procedure

---

**Fig. 3.** Pseudo code of AOA**Fig. 4.** Flowchart of AOA

### 3. Results and Discussion

Initially, the PID controller is tuned using the AOA method, as discussed in Section 2. The tuned PID controller's performance in the buck converter is then compared in terms of its robustness against input voltage disturbances and load changes. The method to evaluate the disturbance rejection capabilities of the closed-loop DC-DC buck converter is referred to paper [20], which a voltage disturbance was introduced after  $5 \times 10^{-6}$  seconds, resulting in a 20% voltage drop from the

reference voltage. Additionally, the buck converter's robustness was assessed by subjecting it to load changes of  $\pm 20\%$  to further verify its disturbance rejection capabilities which are similar to paper [20].

### 3.1. Comparison Algorithms

This study specifically concentrates on the AOA for the purpose of tuning the parameters of the PID controller. Other optimization algorithms like the Hybrid Nelder-Mead Method (AEONM), Artificial Ecosystem-Based Optimization (AEO), Differential Evolution (DE), and Particle Swarm Optimizer (PSO) are compared to AOA because they all belong to candidate-based optimization methods, which rely on a set of candidates to seek the best solution. The PID controller parameter values tuning results by AEONM, AEO, DE, and PSO were directly taken from the paper [20]. Fairly speaking, AOA employed the same upper and lower PID controller parameter limits, population size, and maximum iteration as in the study done in [20]. Maximum iterations were set at 50 with a population size of 24. The PID controller parameter's upper and lower limits are displayed in Table 2.

Following 25 independent runs of the method, the optimal PID controller gain settings were determined by the lowest objective function value. Table 3 displays the lowest objective function value and PID parameters that were tuned by each algorithm in the study.

**Table 2.** Upper and lower limit of PID controller

Parameter	$K_p$	$K_i$	$K_d$
Lower bound	1	0.01	0.001
Upper bound	50	10	0.01

**Table 3.** Result of each algorithm

Algorithm	$J$	$K_p$	$K_i$	$K_d$
AOA	4.6845e-07	44.0089	0.01	0.01
AEONM [20]	4.8016e-07	16.8278	1.1742	0.00992
AEO [20]	4.9920e-07	33.1153	7.9506	0.00943
DE [20]	5.6191e-07	27.6235	1.3043	0.00873
PSO [20]	5.6805e-07	37.1502	3.7255	0.00821

The gain of the PID controller is obtained by substituting the PID parameters from Table 3 into (3). Then by using (4), the closed-loop transfer function of the DC-DC buck converter can then be derived and is presented in equation (17) to (21).

$$TF_{AOA} = \frac{1.296s^5 + 7864s^4 + 2.247 \times 10^7 s^3 + 5.704 \times 10^{10} s^2 + 1.296 \times 10^7 s}{3.6 \times 10^{-7} s^6 + 1.297s^5 + 7872s^4 + 2.248 \times 10^7 s^3 + 5.707 \times 10^{10} s^2 + 1.296 \times 10^7 s} \quad (17)$$

$$TF_{AEONM} = \frac{1.286s^5 + 4324s^4 + 1.649 \times 10^7 s^3 + 2.181 \times 10^{10} s^2 + 1.522 \times 10^9 s}{3.6 \times 10^{-6} s^6 + 1.287s^5 + 4332s^4 + 1.650 \times 10^7 s^3 + 2.185 \times 10^{10} s^2 + 1.522 \times 10^9 s} \quad (18)$$

$$TF_{AEO} = \frac{1.222s^5 + 6329s^4 + 1.938 \times 10^7 s^3 + 4.292 \times 10^{10} s^2 + 1.030 \times 10^{10} s}{3.6 \times 10^{-7} s^6 + 1.223s^5 + 6337s^4 + 1.939 \times 10^7 s^3 + 4.296 \times 10^{10} s^2 + 1.030 \times 10^{10} s} \quad (19)$$

$$TF_{DE} = \frac{1.131s^5 + 5466s^4 + 1.728 \times 10^7 s^3 + 3.580 \times 10^{10} s^2 + 1.690 \times 10^9 s}{3.6 \times 10^{-7} s^6 + 1.133s^5 + 5474s^4 + 1.729 \times 10^7 s^3 + 3.584 \times 10^{10} s^2 + 1.690 \times 10^9 s} \quad (20)$$

$$TF_{PSO} = \frac{1.064s^5 + 6588s^4 + 1.867 \times 10^7 s^3 + 4.815 \times 10^{10} s^2 + 4.828 \times 10^9 s}{3.6 \times 10^{-7} s^6 + 1.065s^5 + 6596s^4 + 1.868 \times 10^7 s^3 + 4.818 \times 10^{10} s^2 + 4.828 \times 10^9 s} \quad (21)$$

### 3.2. Disturbance Rejection Analysis

The disturbance rejection analysis was performed at  $t = 5 \times 10^{-6}$  seconds during the system's steady-state operation to mimic real-world conditions. In this analysis, a negative disturbance of 20 percent of the voltage reference was introduced to assess the system's ability to maintain stability and accurately regulate the output under challenging conditions. By subjecting the system to this disturbance, we were able to evaluate its resilience and effectiveness in rejecting external disturbances and maintaining the desired output voltage. The results of this analysis provide valuable insights into the system's robustness and its capability to mitigate the impact of disturbances, contributing to the overall understanding of its performance characteristics. Fig. 5 illustrates the response of the system to the introduced disturbance, comparing the performance of the AOA algorithm with other compared algorithms.

The comprehensive details of the disturbance rejection analysis, including rise time, settling time, voltage overshoot, voltage peak value, and steady-state error, are presented in Table 4.

It is evident from Fig. 4 and Table 4 that the buck converter with AOA-based PID controller exhibits exceptional performance in quickly restoring the system back to the desired voltage after the disturbance occurs. It demonstrates its effectiveness in efficiently mitigating the impact of the disturbance, leading to rapid response from the desired voltage level. In comparison to the other buck converters, the buck converter with AOA-based PID controller outperforms them by achieving the fastest recovery time and demonstrating superior disturbance rejection capabilities. It exhibits a small overshoot percentage, which, while not the lowest, is still sufficiently small for practical applications. In real-world scenarios, this overshoot percentage can be considered as within the acceptable tolerance range for the desired voltage, and it does not have a significant impact on the load. This is particularly crucial in applications like computers, where voltage disturbances must be quickly rejected to minimize their impact on the computer's operation.

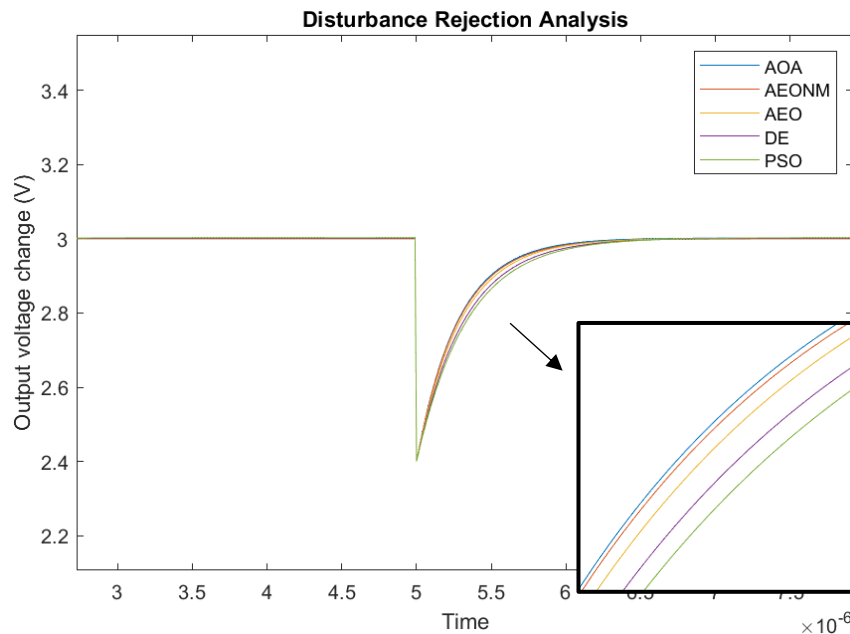


Fig. 5. Disturbance rejection demonstration of buck converter

Table 4. Disturbance rejection analysis of buck converter

Algorithm	Rise time (s)	Settling time (s)	Overshoot (%)	Peak value (V)	Steady-state error (V)
AOA	6.0163e-07	1.0405e-06	0.0741	3.0022	0
AEONM	6.1521e-07	1.0951e-06	0	3.0000	0
AEO	6.4060e-07	1.1165e-06	0.0527	3.0016	0
DE	6.9284e-07	1.2106e-06	0.0459	3.0014	0
PSO	7.2999e-07	1.2536e-06	0.0939	3.0028	0

### 3.3. Robustness on Load Change Analysis

The robustness of the system to load changes is a crucial aspect to evaluate its performance in real-world scenarios. In this analysis, a load change of 1.2 ohms with a variation of  $\pm 20\%$  was introduced to examine the system's response and stability. The system's ability to handle load changes was assessed by observing the transient response and its ability to recover to the desired operating point. The AOA algorithm, along with the compared algorithms, was subjected to this load variation, and their performances were evaluated.

The results in [Table 5](#) indicated that the AOA algorithm exhibited remarkable robustness in dealing with the load change. It effectively adapted to the new load conditions and quickly adjusted the control parameters to maintain the desired output voltage. The system demonstrated a stable response with minimal overshoot and a fast-settling time, ensuring that the voltage remained within an acceptable range.

**Table 5.** Load change analysis of buck converter

Rate of change (%)	Algorithm	Rise time (s)	Settling time (s)	Overshoot (%)	Peak value (V)	Steady-state error (V)
-20	AOA	6.0296e-07	1.0470e-06	0.0626	3.0019	0
-20	AEONM	6.1660e-07	1.1030e-06	0	2.9996	0
-20	AEO	6.4210e-07	1.1242e-06	0.0406	3.0012	0
-20	DE	6.9456e-07	1.2197e-06	0.0328	3.0010	0
-20	PSO	7.3190e-07	1.2629e-06	0.0800	3.0024	0
Rate of change (%)	Algorithm	Rise time (s)	Settling time (s)	Overshoot (%)	Peak value (V)	Steady-state error (V)
20	AOA	6.0076e-07	1.0362e-06	0.0817	3.0025	0
20	AEONM	6.1429e-07	1.0898e-06	0.0076	3.0002	0
20	AEO	6.3960e-07	1.1114e-06	0.0608	3.0018	0
20	DE	6.9168e-07	1.2046e-06	0.0547	3.0016	0
20	PSO	7.2872e-07	1.2475e-06	0.1032	3.0031	0

During the robustness analysis with a 20% load change, the AOA-based PID controller continues to demonstrate the best performance among all controllers. It exhibits the lowest rise time and settling time while maintaining a small voltage overshoot. These findings suggest that the AOA-based PID controller adeptly manages load fluctuations, ensuring stable and precise control of the buck converter system. This makes it well-suited for deployment in renewable energy systems that often contend with challenges related to load variations.

The percentage changes of each parameter during the robustness analysis are presented in [Table 6](#). [Table 6](#) provides valuable insights into how the PID controller responds to the load changes and indicates the controller's ability to maintain stable performance under varying conditions.

**Table 6.** Buck converter performance change analysis

Algorithm	-20% load variation			+20% load variation		
	Change of rise time	Change of settling time	Change of overshoot percent	Change of rise time	Change of settling time	Change of overshoot percent
AOA	+0.2194%	+0.7385%	-0.0114%	-0.1463%	-0.4099%	0.0076%
AEONM	+0.2400%	+0.7532%	0%	-0.1498%	-0.4797%	0.0076%
AEO	+0.2336%	+0.6893%	-0.0122%	-0.1561%	-0.4557%	0.0081%
DE	+0.2489%	+0.7532%	-0.0131%	-0.1664%	-0.4934%	0.0088%
PSO	+0.2608%	+0.7385%	-0.0139%	-0.1744%	-0.4871%	0.0093%

These results highlight the superior robustness of the AOA-based PID controller compared to other optimization algorithms, making it a promising choice for applications where stability and accurate response during load changes are crucial. Overall, the robustness analysis demonstrated that the AOA algorithm can maintain system stability and ensure accurate control even in the presence of

significant load changes. This further solidifies its effectiveness and reliability in practical applications where robust performance is paramount.

### 3.4. Frequency Analysis

Frequency analysis involves simulating the buck converter's performance under complex disturbance signals and high-frequency ripple voltage inputs. The phase margin in this analysis is utilized to determine the maximum stable operating frequency of the buck converter. Additionally, bandwidth evaluation is employed to assess the converter's overall performance, with a higher bandwidth indicating a wider operating range. Frequency analysis is essential in verifying the stability and efficiency of the PID controller for the buck converter. It allows evaluating how well the controller handles complex disturbances and varying voltage ripples, ensuring the converter's stable operation. The Fig. 6 and Table 7 present the outcomes of the frequency analysis for the buck converter under the influence of various PID controllers.

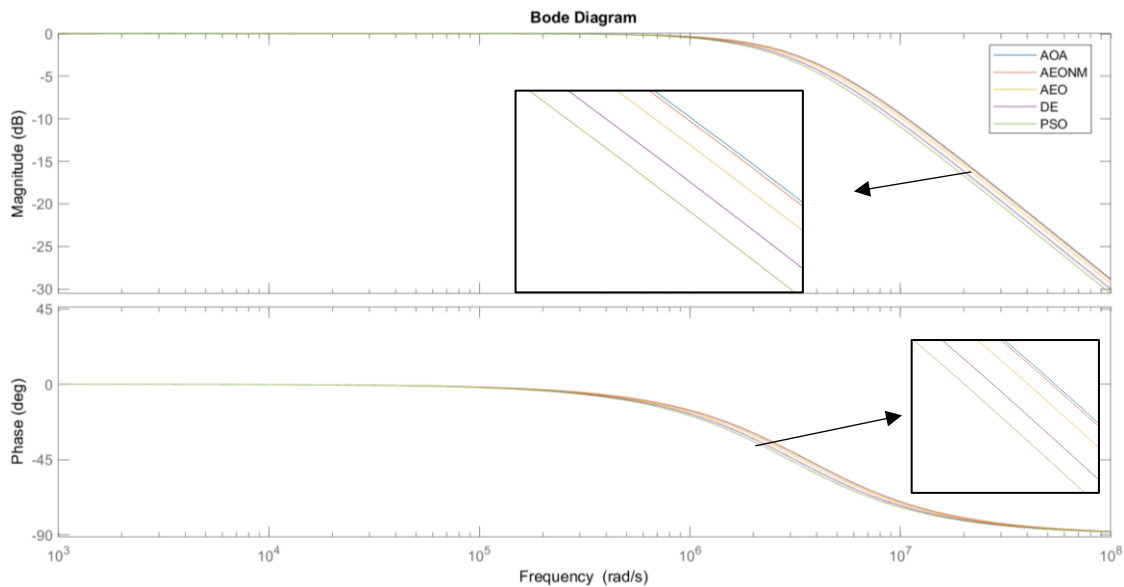


**Fig. 6.** Disturbance rejection demonstration of buck converter

Fig. 6 illustrates that the buck converter with the AOA-based PID controller exhibits the least magnitude dB drop and phase delay degree at the same frequency. This characteristic enhances the converter's immunity to common electrical noise and interference, making it more robust in noisy environments.

**Table 7.** Frequency response analysis

Algorithm	Gain margin (dB)	Phase margin (degree)	Bandwidth (Hz)
AOA	Inf	177.7726	3.5942e+06
AEONM	Inf	-180	3.5628e+06
AEO	Inf	178.1149	3.3886e+06
DE	Inf	178.2405	3.1369e+06
PSO	Inf	177.4863	2.9515e+06

The analysis from Table 7 demonstrates that the buck converter with the AOA-based PID controller has the widest range of bandwidth, indicating its enhanced robustness and ability to handle a broader range of frequencies effectively. This wider bandwidth allows the AOA-based PID controller to respond more efficiently to various disturbances and ripple voltage inputs, ensuring stable and reliable operation of the buck converter under challenging conditions. The findings further validate the effectiveness of the AOA-based PID controller for regulating buck converters in practical scenarios, such as telecommunications, where challenges like fluctuating voltage due to high electromagnetic interference (EMI) are prevalent.

#### 4. Conclusion

The study's conclusion provides a concise summary of the research findings. It highlights the effectiveness of the Archimedes optimization algorithm (AOA) in tuning a PID controller for a buck converter. The superiority of the AOA-based PID controller in terms of disturbance rejection and load change robustness compared to other algorithms is emphasized. The conclusion also emphasizes the stability and adaptability of the AOA-based controller, particularly in handling the buck converter's nonlinear characteristics and varying operating conditions. The study's contribution in showcasing the AOA-based PID controller's resilience to high-frequency disturbances through frequency analysis is highlighted. While the conclusion acknowledges the potential of AOA in broader applications beyond DC-DC converters, it could be strengthened by discussing potential challenges or limitations associated with AOA's application in different scenarios. Additionally, suggesting specific areas of future research beyond converters where AOA could be applied would enhance the conclusion's comprehensiveness.

In terms of future research, the AOA has potential for broader application beyond the DC-DC converter studies conducted in recent years. For instance, the AOA could be employed in analyzing other types of converters like boost converter, buck-boost converter, and flyback converter. AOA also can be used to analyze other modified DC-DC converters like Single-Inductor Multiple-Output DC-DC Converter. Additionally, the AOA's usefulness extends beyond just DC-DC converters and could be explored for addressing various real-world engineering challenges.

**Author Contribution:** All authors contributed equally to the main contributor to this paper. All authors read and approved the final paper.

**Funding:** This research received no external funding.

**Conflicts of Interest:** The authors declare no conflicts of interest.

#### References

- [1] O. Saleem, F. G. Awan, K. Mahmood-ul-Hasan, and M. Ahmad, "Self-adaptive fractional-order LQ-PID voltage controller for robust disturbance compensation in DC-DC buck converters," *International Journal of Numerical Modelling: Electronic Networks, Devices and Fields*, vol. 33, no. 4, Jul. 2020, <https://doi.org/10.1002/jnm.2718>.
- [2] M. W. Alim, N. A. Windarko, and R. Rakhmawati, "Fuzzy Logic Control Design on Buck Converter For Thermo Electric Air Cooler Power Supply," *JAREE (Journal on Advanced Research in Electrical Engineering)*, vol. 4, no. 2, Oct. 2020, <https://doi.org/10.12962/j25796216.v4.i2.137>.
- [3] K. S. Jyothi, "Battery Charging from Solar using Buck Converter with MPPT," *Int. J. Res. Appl. Sci. Eng. Technol.*, vol. 9, no. VI, pp. 3490–3493, Jun. 2020, <https://doi.org/10.22214/ijraset.2021.35919>.
- [4] T. A. Tulong, M. R. H. Chowdhury, M. T. U. -N. Kono, M. R. Uddin and M. Hasan, "Designing a Bidirectional Isolated DC/DC Converter for EV with Power Back Operation for Efficient Battery Charging During Neutral Run," *2022 International Conference on Energy and Power Engineering (ICEPE)*, pp. 1-5, 2022, <https://doi.org/10.1109/ICEPE56629.2022.10044891>.
- [5] A. Garg and M. Das, "High Efficiency Three Phase Interleaved Buck Converter for Fast Charging of EV," *2021 1st International Conference on Power Electronics and Energy (ICPEE)*, pp. 1-5, 2021, <https://doi.org/10.1109/ICPEE50452.2021.9358486>.
- [6] N. E. Zakzouk and R. A. Ibrahim, "Modelling and Performance Analysis of a Buck Converter Featuring Continuous Input/Continuous Output Current for Wind Energy-DC Microgrid," *2022 6th International Conference on Green Energy and Applications*, pp. 127–132, 2022, <https://doi.org/10.1109/ICGEA54406.2022.9792031>.
- [7] M. R. K. Shagor, A. J. Mahmud, M. M. Nishat, F. Faisal, M. H. Mithun, and M. A. Khan, "Firefly Algorithm Based Optimized PID Controller for Stability Analysis of DC-DC SEPIC Converter," *2021*

- IEEE 12th Annual Ubiquitous Computing, Electronics and Mobile Communication Conference*, pp. 957–963, 2021, <https://doi.org/10.1109/UEMCON53757.2021.9666555>.
- [8] A. Sedehi and M. Mirjafari, “Robust Optimal Controller for Buck Converter under Parametric Uncertainty: An LQR Approach,” *2022 13th Power Electronics, Drive Systems, and Technologies Conference*, pp. 101–106, 2022, <https://doi.org/10.1109/PEDSTC53976.2022.9767317>.
- [9] M. Csizmadia and M. Kuczmann, “Design of LQR controller for GaN based Buck converter,” *Pollack Periodica*, vol. 15, no. 2, pp. 37–48, Aug. 2020, <https://doi.org/10.1556/606.2020.15.2.4>.
- [10] O. Saleem and M. Rizwan, “Performance optimization of LQR-based PID controller for DC-DC buck converter via iterative-learning-tuning of state-weighting matrix,” *International Journal of Numerical Modelling: Electronic Networks, Devices and Fields*, vol. 32, no. 3, p. e2572, May 2019, <https://doi.org/10.1002/jnm.2572>.
- [11] H. B. Yuan and Y. B. Kim, “Equivalent input disturbance observer-based ripple-free deadbeat control for voltage regulation of a DC–DC buck converter,” *IET Power Electronics*, vol. 12, no. 12, pp. 3272–3279, Oct. 2019, <https://doi.org/10.1049/iet-pe.2019.0652>.
- [12] A. Iskhakov, Y. Portnoy, S. Skovpen, and D. Gladkiy, “Direct Deadbeat Control of a Buck Converter,” *IECON 2019 - 45th Annual Conference of the IEEE Industrial Electronics Society*, pp. 347–352, Oct. 2019, <https://doi.org/10.1109/IECON.2019.8927163>.
- [13] L. T. Rasheed, “Performance of the adaptive sliding mode control scheme for output voltage control of the DC/DC buck converter system,” *IOP Conf. Ser. Mater. Sci. Eng.*, vol. 881, no. 1, Aug. 2020, <https://doi.org/10.1088/1757-899X/881/1/012118>.
- [14] S. Vadi and R. Bayındır, “Performance Enhancement of SMC Based Buck Converter under Variable Conditions by Particle Swarm Optimization Algorithm,” *2022 3rd International Conference on Smart Grid and Renewable Energy (SGRE)*, pp. 1-8, 2022, <https://doi.org/10.1109/SGRE53517.2022.9774271>.
- [15] M. Hassan, C. L. Su, F. Z. Chen, and K. Y. Lo, “Adaptive Passivity-Based Control of a DC-DC Boost Power Converter Supplying Constant Power and Constant Voltage Loads,” *IEEE Transactions on Industrial Electronics*, vol. 69, no. 6, pp. 6204–6214, Jun. 2022, <https://doi.org/10.1109/TIE.2021.3086723>.
- [16] F. M. Serra, G. L. Magaldi, W. Gil-González, and O. Montoya, “Passivity-Based PI Controller of a Buck Converter for Output Voltage Regulation,” *2020 IEEE ANDESCON*, pp. 1-6, 2020, <https://doi.org/10.1109/ANDESCON50619.2020.9271976>.
- [17] Y. Chen, K. Bai, and Z. Liu, “An approximation time optimal control approach for DC-DC buck converter,” *International Journal of Wireless and Mobile Computing*, vol. 20, no. 3, pp. 290–296, 2021, <https://doi.org/10.1504/IJWMC.2021.115663>.
- [18] N. D. Bhat, D. B. Kanse, S. D. Patil, and S. D. Pawar, “DC/DC Buck Converter Using Fuzzy Logic Controller,” *2020 5th International Conference on Communication and Electronics Systems (ICCES)*, pp. 182-187, 2020, <https://doi.org/10.1109/ICCES48766.2020.9138084>.
- [19] R. M. Brisilla, K. Jnaneswara Venkata Ramana, and M. M. Rao, “Output Voltage Regulation of DC to DC Buck Converter using Integral SMC,” *2019 Innovations in Power and Advanced Computing Technologies (i-PACT)*, pp. 1-5, 2019, <https://doi.org/10.1109/i-PACT44901.2019.8960057>.
- [20] D. Izci, B. Hekimoğlu, and S. Ekinçi, “A new artificial ecosystem-based optimization integrated with Nelder-Mead method for PID controller design of buck converter,” *Alexandria Engineering Journal*, vol. 61, no. 3, pp. 2030–2044, Mar. 2022, <https://doi.org/10.1016/j.aej.2021.07.037>.
- [21] K. S. Reddy, R. Jeyasenthil, and T. Kobaku, “QFT Approach to Robust Control of DC-DC Buck Converter,” *2022 IEEE International Conference on Power Electronics, Drives and Energy Systems (PEDES)*, pp. 1-6, 2022, <https://doi.org/10.1109/PEDES56012.2022.10080328>.
- [22] J. Zhang, S. Li, C. K. Ahn, and Z. Xiang, “Sampled-data output voltage regulation for a DC–DC buck converter nonlinear system with actuator and sensor failures,” *Nonlinear Dyn.*, vol. 99, no. 2, pp. 1243–1252, Jan. 2020, <https://doi.org/10.1007/s11071-019-05350-6>.

- 
- [23] J. Wang, C. Jurgenson, N. Allu, and A. Toding, "Tuning with Ziegler Nichols Method for Design PID Controller At Rotate Speed DC Motor," *IOP Conf. Ser. Mater. Sci. Eng.*, vol. 846, no. 1, p. 012046, May 2020, <https://doi.org/10.1088/1757-899X/846/1/012046>.
- [24] Z. Wang, S. Qiu, R. Song, X. Wang, B. Zhu, and B. Li, "Research on PID parameter tuning of coordinated control for ultra-supercritical units based on Ziegler Nichols method," *Proceedings of 2019 IEEE 3rd Advanced Information Management, Communicates, Electronic and Automation Control Conference*, pp. 1155–1158, Oct. 2019, <https://doi.org/10.1109/IMCEC46724.2019.8984069>.
- [25] K. H. Tseng, M. Y. Chung, C. Y. Chang, C. L. Hsieh, Y. K. Tseng, "Parameter optimization of nanosilver colloid prepared by electrical spark discharge method using Ziegler-Nichols method," *Journal of Physics and Chemistry of Solids*, vol. 148, p. 109650, 2021, <https://doi.org/10.1016/j.jpcs.2020.109650>.
- [26] A. R. Utami, R. J. Yuniar, A. Giyantara, and A. D. Saputra, "Cohen-Coon PID Tuning Method for Self-Balancing Robot," *2022 International Symposium on Electronics and Smart Devices (ISESD)*, pp. 1-5, 2022, <https://doi.org/10.1109/ISESD56103.2022.9980830>.
- [27] A. Makalesi and A. E. Taşören, "Design and Realization of Online Auto Tuning PID Controller Based on Cohen-Coon Method," *European Journal of Science and Technology*, vol. 24, no. 24, pp. 234–239, Apr. 2021, <https://doi.org/10.31590/ejosat.897727>.
- [28] A. R. Utami, R. J. Yuniar, A. Giyantara and A. D. Saputra, "Cohen-Coon PID Tuning Method for Self-Balancing Robot," *2022 International Symposium on Electronics and Smart Devices (ISESD)*, pp. 1-5, 2022, <https://doi.org/10.1109/ISESD56103.2022.9980830>.
- [29] W. Bu *et al.*, "Performance analysis of PID control in DC Brushless motor using trial and error method," *IOP Conf. Ser. Mater. Sci. Eng.*, vol. 1098, no. 4, p. 042027, Mar. 2021, <https://doi.org/10.1088/1757-899X/1098/4/042027>.
- [30] C. Khongprasongsiri, P. Areerob, S. Boonto, and W. Vongsantivanich, "Hardware Implementation of PID Autotuning with Efficient Particle Swarm Optimization," *2023 20th International Conference on Electrical Engineering/Electronics, Computer, Telecommunications and Information Technology (ECTI-CON)*, pp. 1-4, 2023, <https://doi.org/10.1109/ECTI-CON58255.2023.10153278>.
- [31] M. M. Nishat, F. Faisal, A. J. Evan, Md. M. Rahaman, Md. S. Sifat, and H. M. F. Rabbi, "Development of Genetic Algorithm (GA) Based Optimized PID Controller for Stability Analysis of DC-DC Buck Converter," *Journal of Power and Energy Engineering*, vol. 8, no. 9, pp. 8–19, 2020, <https://doi.org/10.4236/jpee.2020.89002>.
- [32] D. Izci, S. Ekinci, and B. Hekimoğlu, "A novel modified Lévy flight distribution algorithm to tune proportional, integral, derivative and acceleration controller on buck converter system," *Transactions of the Institute of Measurement and Control*, vol. 44, no. 2, pp. 393–409, Aug. 2021, <https://doi.org/10.1177/01423312211036591>.
- [33] B. Hekimoğlu, S. Ekinci, and S. Kaya, "Optimal PID Controller Design of DC-DC Buck Converter using Whale Optimization Algorithm," *2018 International Conference on Artificial Intelligence and Data Processing (IDAP)*, pp. 1-6, 2018, <https://doi.org/10.1109/IDAP.2018.8620833>.
- [34] M. R. K. Shagor, A. J. Mahmud, M. M. Nishat, F. Faisal, M. H. Mithun, and M. A. Khan, "Firefly Algorithm Based Optimized PID Controller for Stability Analysis of DC-DC SEPIC Converter," *2021 IEEE 12th Annual Ubiquitous Computing, Electronics & Mobile Communication Conference (UEMCON)*, pp. 0957-0963, 2021, <https://doi.org/10.1109/UEMCON53757.2021.9666555>.
- [35] M. Huang, M. Tian, Y. Liu, Y. Zhang, and J. Zhou, "Parameter optimization of PID controller for water and fertilizer control system based on partial attraction adaptive firefly algorithm," *Scientific reports*, vol. 12, no. 1, p. 12182, 2022, <https://doi.org/10.1038/s41598-022-16425-7>.
- [36] S. Ekinci, B. Hekimoğlu, E. Eker, and D. Sevim, "Hybrid Firefly and Particle Swarm Optimization Algorithm for PID Controller Design of Buck Converter," *2019 3rd International Symposium on Multidisciplinary Studies and Innovative Technologies (ISMSIT)*, pp. 1-6, 2019, <https://doi.org/10.1109/ISMSIT.2019.8932733>.
- [37] M. E. Çimen, Z. B. Garip, and A. F. Boz, "Chaotic flower pollination algorithm based optimal PID controller design for a buck converter," *Analog Integrated Circuits and Signal Processing*, vol. 107, no. 2, pp. 281–298, May 2021, <https://doi.org/10.1007/s10470-020-01751-5>.
-

- [38] B. Hekimoğlu and S. Ekinçi, "Optimally designed PID controller for a DC-DC buck converter via a hybrid whale optimization algorithm with simulated annealing," *Electrica*, vol. 20, no. 1, pp. 19–27, Jan. 2020, <https://doi.org/10.5152/electrica.2020.19034>.
- [39] L. T. Rasheed, "Bat Algorithm Based an Adaptive PID Controller Design for Buck Converter Model," *Journal of Engineering*, vol. 26, no. 7, pp. 62–82, Jul. 2020, <https://doi.org/10.31026/j.eng.2020.07.05>.
- [40] N. F. Nanyan, M. A. Ahmad, and B. Hekimoğlu, "Optimal Pid Controller for the Dc-Dc Buck Converter Using the Improved Sine Cosine Algorithm," *SSRN Electronic Journal*, 2023, <https://doi.org/10.2139/ssrn.4388992>.
- [41] S. M. Ghamari, H. G. Narm, and H. Mollaei, "Fractional-order fuzzy PID controller design on buck converter with antlion optimization algorithm," *IET Control Theory & Applications*, vol. 16, no. 3, pp. 340–352, Feb. 2022, <https://doi.org/10.1049/cth2.12230>.
- [42] P. Warriar and P. Shah, "Optimal Fractional PID Controller for Buck Converter Using Cohort Intelligent Algorithm," *Applied System Innovation*, vol. 4, no. 3, p. 50, Aug. 2021, <https://doi.org/10.3390/asi4030050>.
- [43] X. Li, X. Zhang, and F. Lin, "Multi-Objective Design of Output LC Filter for Buck Converter via the Coevolving-AMOSA Algorithm," *IEEE Access*, vol. 9, pp. 11884–11894, 2021, <https://doi.org/10.1109/ACCESS.2020.3034361>.
- [44] M. Z. Mohd Tumari, M. A. Ahmad, M. H. Suid, and M. R. Hao, "An Improved Marine Predators Algorithm-Tuned Fractional-Order PID Controller for Automatic Voltage Regulator System," *Fractal and Fractional*, vol. 7, no. 7, p. 561, Jul. 2023, <https://doi.org/10.3390/fractalfract7070561>.
- [45] R. Singh and R. Kaur, "A Novel Archimedes Optimization Algorithm with Levy Flight for Designing Microstrip Patch Antenna," *Arabian Journal for Science and Engineering*, vol. 47, no. 3, pp. 3683–3706, Mar. 2022, <https://doi.org/10.1007/s13369-021-06307-x>.
- [46] L. Chen and T. Rezaei, "A New Optimal Diagnosis System for Coronavirus (COVID-19) Diagnosis Based on Archimedes Optimization Algorithm on Chest X-Ray Images," *Computational Intelligence and Neuroscience*, vol. 2021, 2021, <https://doi.org/10.1155/2021/7788491>.
- [47] W. Aribowo, S. Muslim, B. Suprianto, S. I. Haryudo, and A. C. Hermawan, "Intelligent Control of Power System Stabilizer Based on Archimedes Optimization Algorithm – Feed Forward Neural Network," *International Journal of Intelligent Engineering and Systems*, vol. 14, no. 3, pp. 43–53, Jun. 2021, <https://doi.org/10.22266/ijies2021.0630.05>.
- [48] A. Fathy, A. G. Alharbi, S. Alshammari, and H. M. Hasanien, "Archimedes optimization algorithm based maximum power point tracker for wind energy generation system," *Ain Shams Engineering Journal*, vol. 13, no. 2, p. 101548, Mar. 2022, <https://doi.org/10.1016/j.asej.2021.06.032>.
- [49] E. H. Houssein, B. E. din Helmy, H. Rezk, and A. M. Nassef, "An enhanced Archimedes optimization algorithm based on Local escaping operator and Orthogonal learning for PEM fuel cell parameter identification," *Engineering Applications of Artificial Intelligence*, vol. 103, p. 104309, Aug. 2021, <https://doi.org/10.1016/j.engappai.2021.104309>.
- [50] F. A. Hashim, K. Hussain, E. H. Houssein, M. S. Mabrouk, and W. Al-Atabany, "Archimedes optimization algorithm: a new metaheuristic algorithm for solving optimization problems," *Applied Intelligence*, vol. 51, no. 3, pp. 1531–1551, Mar. 2021, <https://doi.org/10.1007/s10489-020-01893-z>.